

DEVELOPMENT OF MUCOADHESIVE BILIOSOME NANOPARTICLES FOR ENHANCED
GASTROINTESTINAL ABSORPTION OF CORDYCEPIN



A Thesis Submitted in Partial Fulfillment of the Requirements
for the Degree of Master of Science in Pharmaceutical Sciences and Technology

Common Course

FACULTY OF PHARMACEUTICAL SCIENCES

Chulalongkorn University

Academic Year 2019

Copyright of Chulalongkorn University

การพัฒนาอนุภาคนาโนบิโกลินไอโซมที่มีคุณสมบัติยึดติดเยื่อเมือกเพื่อเพิ่มการดูดซึมสารคอร์ไตซิปีน
ผ่านทางเดินอาหาร



วิทยานิพนธ์นี้เป็นส่วนหนึ่งของการศึกษาตามหลักสูตรปริญญาวิทยาศาสตรมหาบัณฑิต
สาขาวิชาเภสัชศาสตร์และเทคโนโลยี ไม่สังกัดภาควิชา/เทียบเท่า
คณะเภสัชศาสตร์ จุฬาลงกรณ์มหาวิทยาลัย
ปีการศึกษา 2562
ลิขสิทธิ์ของจุฬาลงกรณ์มหาวิทยาลัย

วรุศม์ เก่งกิตติภัทร : การพัฒนาอนุภาคนาโนบิโลนิโอโซมที่มีคุณสมบัติยึดติดเยื่อเมือก เพื่อเพิ่มการดูดซึมสารคอร์ไดซิปีนผ่านทางเดินอาหาร. (DEVELOPMENT OF MUCOADHESIVE BILONIOSOME NANOPARTICLES FOR ENHANCED GASTROINTESTINAL ABSORPTION OF CORDYCEPIN) อ.ที่ปรึกษาหลัก : รศ. ดร. วรัญญ พูลเจริญ, อ.ที่ปรึกษาร่วม : ดร.คทาวัธ นามติ

ถั่งเช่า (Cordyceps) เป็นสมุนไพรที่มีการใช้อย่างแพร่หลายในปัจจุบัน โดยมีสารออกฤทธิ์ที่สำคัญคือ สารคอร์ไดซิปีน (Cordycepin) โดยเป็นอนุพันธ์ของสารอะดีโนซีน (adenosine) ซึ่งมีฤทธิ์เภสัชวิทยาหลายประการ ตัวอย่างเช่น ฤทธิ์ในการเหนี่ยวนำให้เกิดกระบวนการอะพอพโทซิส และยับยั้งการเจริญเติบโตของเซลล์มะเร็ง ฤทธิ์ในการต้านอนุมูลอิสระ ช่วยเพิ่มสมรรถนะทางเพศ อย่างไรก็ตาม ในทางปฏิบัติการนำสารคอร์ไดซิปีนเข้าสู่ร่างกายโดยวิธีประทานยังเป็นข้อจำกัดเนื่องจากชีวปริมาณออกฤทธิ์มีค่าน้อยมาก ด้วยเหตุผลดังกล่าว ผู้วิจัยจึงพัฒนาระบบนำส่งยาอนุภาคนาโนขึ้น เพื่อเพิ่มประสิทธิภาพในการนำส่งยาในระบบทางเดินอาหาร โดยใช้เกลือน้ำดีมาเป็นส่วนประกอบในการทำลิโปโซม เรียกว่า บิโลนิโอโซม นอกจากนี้ผู้วิจัยยังทั้งเพิ่มโคโคซานเข้าไปห่อหุ้มอนุภาคบิโลนิโอโซม เพื่อเพิ่มคุณสมบัติการติดเยื่อเมือก ซึ่งส่งผลให้ชีวปริมาณออกฤทธิ์สูงขึ้น การสังเคราะห์อนุภาคบิโลนิโอโซมที่ใส่สารคอร์ไดซิปีนทำโดยวิธีฉีดด้วยตัวทำละลาย (เอทานอล) และจึงห่อหุ้มอนุภาคด้วยโคโคซาน ผู้วิจัยได้ทำศึกษาคุณสมบัติทางเคมีฟิสิกส์ และคุณสมบัติทางชีวภาพ เช่น ศึกษาฤทธิ์การต้านมะเร็ง ศึกษาความสามารถในการซึมผ่านของอนุภาคผ่านเซลล์ลำไส้ โดยอนุภาคบิโลนิโอโซมที่สังเคราะห์ขึ้นมีขนาด 150 นาโนเมตร ประสิทธิภาพการกักเก็บยามากกว่า 60% นอกจากนี้อนุภาคดังกล่าวมีฤทธิ์ต้านเซลล์มะเร็ง (HT29) ได้ และจากการห่อหุ้มอนุภาคด้วยโคโคซานพบว่า อนุภาคบิโลนิโอโซมที่ห่อหุ้มด้วยโคโคซานมีคุณสมบัติการติดเยื่อเมือกและสามารถซึมผ่านผนังลำไส้ มากกว่าอนุภาคบิโลนิโอโซมที่ไม่ได้ห่อหุ้มด้วยโคโคซาน ถึง 3 เท่า ซึ่งนวัตกรรมนาโนที่ผู้วิจัยได้ศึกษานี้ สารคอร์ไดซิปีนที่กักเก็บในระบบนำส่งยาอนุภาคบิโลนิโอโซม จะสามารถพัฒนาต่อเพื่อนำไปใช้เป็นยาเคมีบำบัดสำหรับการรักษา มะเร็งทางเดินอาหารต่อไป

สาขาวิชา	เภสัชศาสตร์และเทคโนโลยี	ลายมือชื่อนิสิต
ปีการศึกษา	2562	ลายมือชื่อ อ.ที่ปรึกษาหลัก
		ลายมือชื่อ อ.ที่ปรึกษาร่วม

6176107933 : MAJOR PHARMACEUTICAL SCIENCES AND TECHNOLOGY

KEYWORD: Cordycepin, Oral administration, Hybrid nanoparticle, Biloniosome

Warut Kengkittipat : DEVELOPMENT OF MUCOADHESIVE BILONIOSOME NANOPARTICLES FOR ENHANCED GASTROINTESTINAL ABSORPTION OF CORDYCEPIN. Advisor: Assoc. Prof. WARANYOO PHOOLCHAROEN, Ph.D. Co-advisor: Katawut Namdee, Ph.D.

Cordycepin, an adenosine analogue, has displayed numerous pharmacological and therapeutic implications including enhanced apoptosis and inhibition of proliferation of cancer cells, antioxidant property and improving sexual activity. However, oral administration of cordycepin has limited practical use due to its poor bioavailability in the intestine. Here, we developed a novel hybrid nanoparticle system for effective delivery of cordycepin in the gastrointestinal tract by using the bile salt-based liposome/niosome hybrid system (designated as biloniosome). In addition, mucoadhesive chitosan biopolymer was coated on the biloniosome nanoparticles to improve the mucoadhesive properties thereby enhancing the drug efficiency. Cordycepin-encapsulated biloniosome nanoparticles were synthesized by solvent (ethanol) injection technique followed by coating with chitosan. The physicochemical characteristics of the prepared nanoparticles were investigated. Their biological activities, such as in vitro anticancer activity and in vitro permeation across the human intestinal barrier were evaluated. We successfully produced hybrid nanoparticles with ~150 nm in diameter and over 60% loading efficiency of cordycepin. The evaluation of hydrodynamic size and zeta-potential indicated that chitosan successfully modified the biloniosome. Interestingly, the hybrid nanoparticles showed potent cytotoxic activity against HT29 cell lines. Our results demonstrated that the chitosan-coated biloniosome.

Field of Study: Pharmaceutical Sciences Student's Signature
and Technology

Academic Year: 2019

Advisor's Signature

Co-advisor's Signature

ACKNOWLEDGEMENTS

This research would not have been successful without the support and assistance from my supporter. I wish to thank all the people whose assistance was a milestone in the completion of this project.

I would first like to thank my thesis advisor Associate Professor Waranyoo Phoolcharoen of the Department of Pharmacognosy & Pharmaceutical Botany, Faculty of Pharmaceutical Sciences, Chulalongkorn University and co-advisor Dr. Katawut Namdee of the National Nanotechnology Center (NANOTEC), National Science and Technology Development Agency (NSTDA). The doors to these advisor offices were always open whenever I ran into a trouble spot or had a question about my research or writing. They consistently allowed this paper to be my own work, but steered me in the right the direction whenever he thought I needed it.

Next, I must express my very profound gratitude to my parents and to my friend for providing me with unfailing support and continuous encouragement throughout my years of study and through the process of researching and writing this thesis. This accomplishment would not have been possible without them. Thank you.

Finally, my thanks also go out to the support I received from Thailand Graduate Institute of Science and Technology Scholarship (TGIST) ; Grant numbers SCA-CO-2561-7042TH, National Science and Technology Development Agency (NSTDA, Thailand) and the 90th Anniversary of Chulalongkorn University Fund (Ratchadaphiseksomphot Endowment Fund) Batch 45 (1/2020), Chulalongkorn University (CU, Thailand) for the financial support.

Warut Kengkittipat

TABLE OF CONTENTS

	Page
.....	iii
ABSTRACT (THAI).....	iii
.....	iv
ABSTRACT (ENGLISH).....	iv
ACKNOWLEDGEMENTS.....	v
TABLE OF CONTENTS.....	vi
LIST OF TABLES.....	ix
List of Figure.....	x
CHAPTER I INTRODUCTION.....	1
CHAPTER II LITERATURE REVIEW.....	4
I. Cordyceps militaris and its major active compounds.....	4
II. Classification of Nanoparticles.....	7
III. Advantages of Nanoparticles.....	7
IV. Methods for construction of nanoparticles.....	8
V. Characterization of nanoparticles.....	8
Physicochemical characterization.....	8
Particle size (Dynamic Light Scattering, Scanning and Transmission Electron Microscopy, Atomic Force Microscopy).....	8
Surface charge.....	9
Biological characterization.....	9
Cell-based assays.....	9

Uptake mechanism.....	9
CHAPTER III MATERIALS AND METHOD.....	13
Materials.....	13
Method.....	13
1. Preparation of biloniosome nanoparticles.....	13
2. Determination of encapsulation efficiency (EE).....	14
3. Physicochemical characterization of biloniosome nanoparticles.....	15
4. Stability in gastrointestinal fluids.....	15
5. Cell culture.....	15
6. Mucoadhesiveness of chitosan-coated biloniosomes.....	16
7. In vitro model of the human intestinal follicle-associated epithelium	17
8. Cell viability.....	18
9. Tumor spheroids	18
10. Gene expression analysis	19
CHAPTER IV RESULTS AND DISCUSSIONS	20
1. Characterizations of biloniosome nanoparticle.....	20
2. Gastric stability	23
3. Mucoadhesive properties	24
4. Permeability assay.....	26
5. Anti-cancer and gene expression analysis	28
CHAPTER V CONCLUSIONS	33
REFERENCES	34
VITA.....	44

LIST OF TABLES

	Page
Table 1 : Components of biliosome nanoparticles.....	14
Table 2 : A series of particle:mucin ratios (v/v) in mucin mixture.....	16



List of Figure

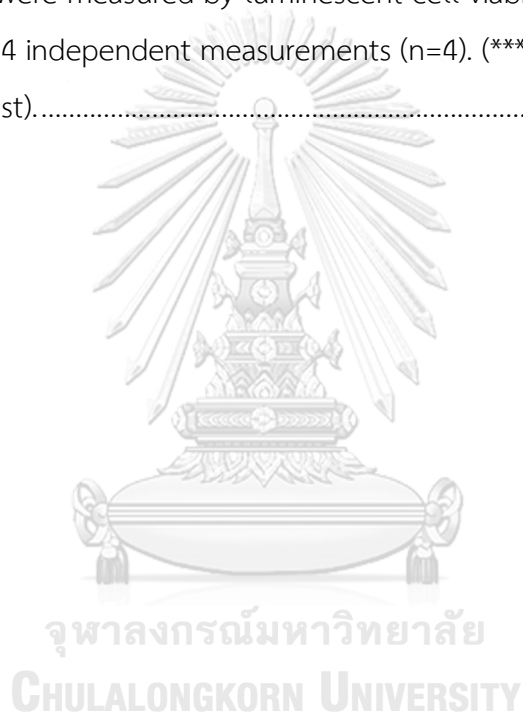
	Page
Figure 1 . Schematic diagram of the preparation of Cordycepin-encapsulated nanoparticles. Cordycepin-encapsulated biloniosomes are fabricated, followed by coating with chitosan polymers.....	3
Figure 2 : Morphological and microscopic identification of <i>Cordyceps militaris</i> and <i>Cordyceps sinensis</i> (A) Crude drugs of <i>Cordyceps militaris</i> (nutrient medium, without larva body; stroma orange-yellow to orange-red). (B) Transverse section of the stroma of <i>Cordyceps militaris</i> (colorless hyphae only) (C) Crude drugs of <i>Cordyceps sinensis</i> (larva body with 8 pairs of feet on the abdomen, 4 pairs apparent in the center; stroma with sterile acuminate apex). (D) Transverse section of the stroma of <i>Cordyceps sinensis</i> (perithecia elliptical to oval, semi-embedded at the surface of the fertile portion of a stroma). [Modified from (Liu, Hu et al. 2011)]	5
Figure 3 : Chemical structure of cordycepin (3'-deoxyadenosine) and adenosine	6
Figure 4 : Pathways of endocytosis. Cellular uptake of large particles is mediated by phagocytosis (a), whereas fluid uptake is facilitated by pinocytosis (b). Different particles can be also internalised through different pathways, including caveolar-mediated endocytosis (c), clathrin-mediated endocytosis (d) and clathrin-independent and caveolin-independent endocytosis (e) (Modified from (Petros and DeSimone 2010)).....	12
Figure 5 : Caco-2 cultivation is established on the apical chamber of a Corning® 12-well plate Transwell inserts (polycarbonate membrane, polystyrene plate, 0.4 µm pore size, 12 mm diameter, Corning®, New York, NY, USA).	17
Figure 6 : Schematic diagram of the chitosan-complexed biloniosome. The negatively charged biloniosome were electrostatically with cationic chitosan polymers to form chitosan- biloniosome complexes.	20
Figure 7 : TEM images of chitosan complexed biloniosome.....	21

- Figure 8 : The optimization of the ratio between chitosan and biloniosome (v/v) by using size and zeta potential. (size; n.s. $p \geq 0.001$; one-way ANOVA with Tukey post test)..... 22
- Figure 9 In vitro gastric stability assay of nanoparticles in simulated gastric fluid (SGF) comprising pepsin at pH 1.2 and incubated at 37 °C for 1 hr. Data represents mean \pm SEM from 3 independent measurements (n=3)..... 24
- Figure 10 : In vitro mucoadhesive assay between biloniosome nanoparticles and purified porcine intestinal mucin. The adhesive properties were observed by the differentiation of size and zeta potential of nanoparticle in mucin mixtures incubated at 37°C for 1 hr. (n.s. $p \geq 0.001$; one-way ANOVA with Tukey post test). Data represents mean \pm SEM from 3 independent measurements (n=3). 25
- Figure 11 : Caco2 cultured transwell assay was established to evaluate the transcytosis of biloniosome nanoparticles. 2 cultured transwell permeability assay for biloniosome nanoparticles. The expression of tight junction protein claudin-5. Green: claudin-5 proteins; Blue: Hoechst, cell nucleus. 27
- Figure 12 : The permeability of nanoparticles were directly evaluated with amount of cordycepin through transwells by HPLC, compared to cordycepin, at 37°C. The solution was collected in bottom wells after 30 min, 1 h, 3 h and 6 h incubation. Data represents mean \pm SEM from 4 independent measurements (n=4)..... 27
- Figure 13 : Effects of cordycepin and biloniosome nanoparticles encapsulated cordycepin on colorectal cancer cell (HT-29). % cell viability. HT-29 cell were treated with nanoparticles for 24 hr. and determined by MTT assay. Data represents mean \pm SEM from 8 independent measurements (n=8)..... 28
- Figure 14, 15 : Cell transcript expression levels of genes regulating cell proliferation and apoptosis. HT-29 cells were untreated or treated for 6 h with 120 $\mu\text{g/ml}$ of (12.) cordycepin or (13.) nanoparticles-encapsulated cordycepin. Total RNA was extracted, DNase-treated, and converted to cDNA. Relative expression levels of CCND1, CDK4, BCL2, BCL-XL, and BAX genes were analyzed by RT-qPCR. Data were normalized to

the GAPDH and RPS13 levels present in the same samples. (***) $p < 0.001$; one-way ANOVA with Tukey post test). 30

Figure 16 : Tumor spheroids were stained by live/dead cell viability dye; dead cells (red-ethidium homodimer-1), live cells (green-Calcein, AM)..... 31

Figure 17 : 3D spheroid assay model of colorectal cancer cell (HT-29). HT-29 cell were seeded and grown in ultra-low attachment round-bottomed plates, after 5 days, then treated with cordycepin encapsulated nanoparticles at 100 ppm for 48 hr. % cell availability were measured by luminescent cell viability assay. Data represents mean \pm SEM from 4 independent measurements (n=4). (***) $p < 0.001$; one-way ANOVA with Tukey post test). 32



CHAPTER I

INTRODUCTION

Cordyceps, a derivative of nucleotide adenosine produced by fungus *Cordyceps militaris*, is widely used in traditional medicines of the Far East (Tuli, Sharma et al. 2013). This compound has been reported to possess various pharmacological effects such as anti-inflammatory, anti-cancer, anti-metastatic, anti-angiogenesis, anti-bacterial and fungal, anti-oxidant, and anti-diabetic effects, making it a appropriate candidate for pharmacological use (Lee, Adrower et al. 2017).

The potential obstacles associated with oral delivery of drugs or bioactive natural compounds can reduce or inhibit the pharmacological activity of the drugs. For example, the acidic pH environment found in the gastrointestinal tract of humans and animals could potentially damage some bioactive compounds (Fricker, Kromp et al. 2010, Bernkop-Schnürch 2013, Thanki, Gangwal et al. 2013). Hence, the orally administered compounds must tolerate the acidic enzymes and survive through the gastrointestinal tract. It is also well-established that, the gastrointestinal epithelium is considered as a physical barrier for bioactive compound absorption into blood circulatory system resulting in inefficient delivery of bioactive compounds into the action site which in turn requires the administration of large doses of such compounds. Therefore, the development of nanotechnology-based drug delivery systems capable of efficient and selective delivering of bioactive compounds to intestine is of important. The general idea behind this concept is that coating of wall material could protect and control the release of active ingredients in the intestine. More interestingly, several strategies have been proposed to enhance the efficacy of orally administered nanoparticles. The more resistant bile salts-containing nanoparticles have been developed by inclusion of bile salts into lipid bilayers constructs (Aburahma 2016). In addition, bioadhesive polymers have been exploited to circumvent the issue of inefficient targeting nanoparticles to mucosal surfaces. Of which, a natural polycationic linear polysaccharide chitosan (CS), has been extensively used in various pharmaceutical and biomedical applications such as for

drug delivery studies due to its excellent biological properties such as mucoadhesiveness, biocompatibility and biodegradability (Cheung, Ng et al. 2015, Ways, Mohammed et al. 2018).

Taken together, we hypothesize that the efficacy of Cordycepin could be improved by nanoencapsulation with bile salts and mucoadhesive characteristic compound. Specifically, implementation of the combination of the aforementioned strategies would improve the stability and therapeutic efficacy of Cordycepin.

The aim of the present study is to investigate the application of nanotechnology-based drug delivery system to enhance the efficacy of orally administered Cordycepin. To achieve this goal, niosome formed by self-association of nonionic surfactants and cholesterol (Ag Seleci, Seleci et al. 2016) were exploited as a nanocarrier for efficient delivery of Cordycepins and the incorporation of bile salts into nanoparticles were exploited to circumvent the issue of nanoparticle degradation in the gastrointestinal tract. Taken together, we used bile salts to formulate the bile salt-based niosome hybrid system (designated as biloniosome) in order to prevent the bioactive compound from enzyme degradation, and to avoid the harsh environment in which the encapsulated particles are exposed in the intestine. Surface modification with chitosan was also attempted in order to circumvent the issue of inefficient targeting nanoparticles to mucosal surfaces.

In this study, we prepare an improved version of cordycepin-encapsulated nanoparticles as schematically shown in **Figure 1**. The physicochemical properties and the stability in simulated gastrointestinal fluids will be analyzed. Their mucoadhesive characteristics, their ability to cross intestinal barriers as well as anticancer activity against colorectal cancers will be also evaluated.

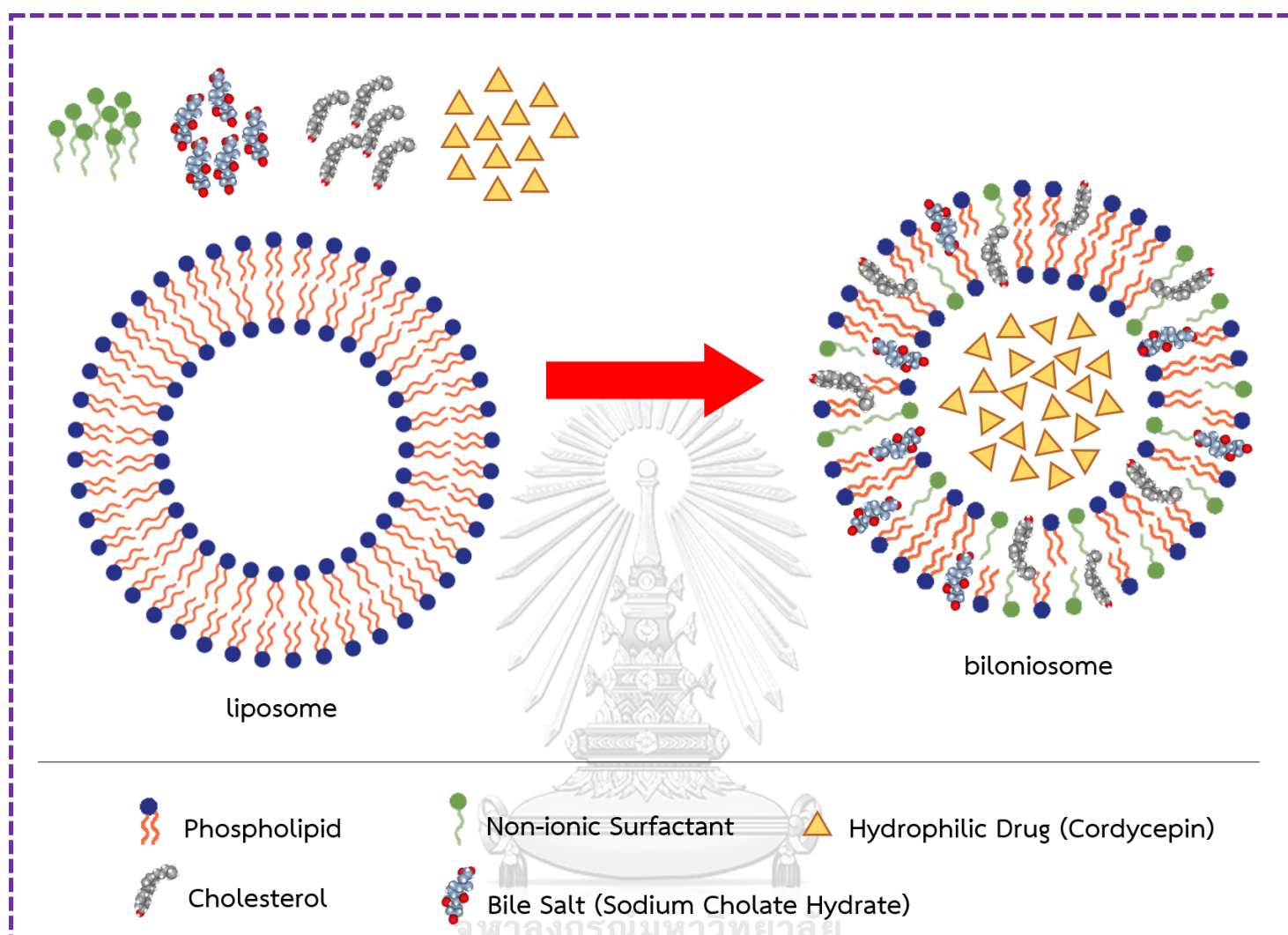


Figure 1 . Schematic diagram of the preparation of Cordycepin-encapsulated nanoparticles. Cordycepin-encapsulated biliosomes are fabricated, followed by coating with chitosan polymers.

CHAPTER II

LITERATURE REVIEW

I. *Cordyceps militaris* and its major active compounds

Cordyceps militaris is a species of fungus in the *Cordyceps* genus, known as "Winter Worm Summer Grass" in English, "Dong Chung Ha Cao" in Korea and "Dong Chong Xia-Cao" in China (Hur 2008), that grows on the larva of insects. *Cordyceps* genus is also found to be rich in useful natural compounds, such as cordycepin, cordycepic acid, ergosterol, polysaccharides, nucleosides and peptides (Yue, Ye et al. 2013). Many previous studies show that *Cordyceps* and its active compounds can have significant effects on a wide range of pharmacological actions, such as anti-inflammatory (Rao, Fang et al. 2010), anti-oxidant (Leung, Zhao et al. 2009), anti-tumour (Lin and Chiang 2008), anti-hyperglycaemic (KIHO, Hui et al. 1993, Kiho, Ookubo et al. 1999), anti- hyper-cholesterolemic (Yamaguchi, Kagota et al. 2000, Koh, Kim et al. 2003), anti-apoptosis (Buenz, Bauer et al. 2005), immunomodulatory (Xu, Peng et al. 1992), nephroprotective (Zhao-Long, Xiao-Xia et al. 2000), and hepatoprotective (Gong, Wang et al. 2000). *Cordyceps militaris*, commonly known as orange caterpillar fungus (Shrestha, Zhang et al. 2012), is one of the most beneficial traditional Chinese medicines (Zheng, Xia et al. 2012, Yue, Ye et al. 2013). This fungi can serve as a cheap substitute of *Ophiocordyceps sinensis* (Lu, Zhi et al. 2019), formerly known as *Cordyceps sinensis*, and Both contain cordycepin.

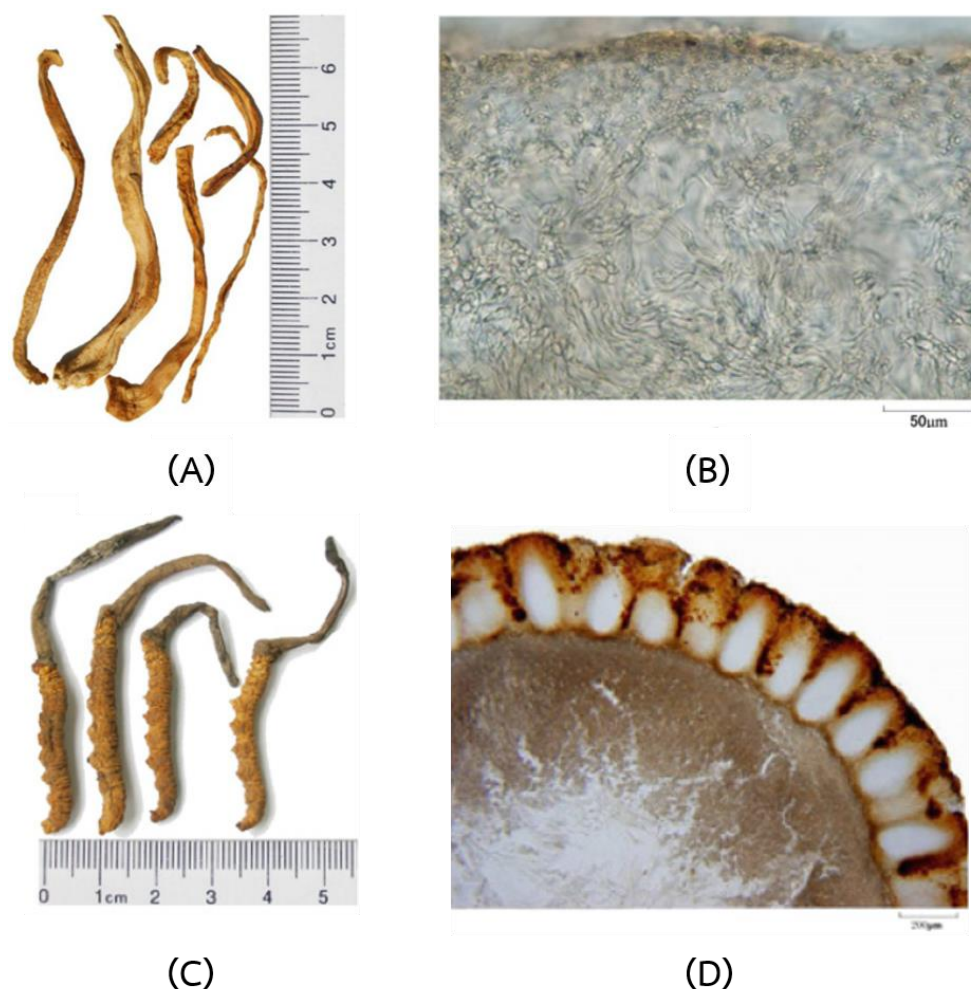


Figure 2 : Morphological and microscopic identification of *Cordyceps militaris* and *Cordyceps sinensis* (A) Crude drugs of *Cordyceps militaris* (nutrient medium, without larva body; stroma orange-yellow to orange-red). (B) Transverse section of the stroma of *Cordyceps militaris* (colorless hyphae only) (C) Crude drugs of *Cordyceps sinensis* (larva body with 8 pairs of feet on the abdomen, 4 pairs apparent in the center; stroma with sterile acuminate apex). (D) Transverse section of the stroma of *Cordyceps sinensis* (perithecia elliptical to oval, semi-embedded at the surface of the fertile portion of a stroma). [Modified from (Liu, Hu et al. 2011)]

Cordycepin is the major bioactive component of Cordyceps. Early in 1950, Cordycepin was first isolated from cultured *Cordyceps militaris* (Cunningham, Manson et al. 1950) and identified as 3'-deoxyadenosine in 1964 (Kaczka, Trenner et al. 1964). Cordycepin results from a 3'-deoxyribose (cordycepose) with a branched carbon chain replacing the ribose of adenosine (Lennon and Suhadolnik 1976). The analysis of cordycepin agreed with the formula $C_{10}H_{13}O_3N_5$ and following studies found that 251 g/mol is the molecular weight of cordycepin with melting points between 230 - 231°C and Cordycepin soluble in water, hot ethanol and methanol, but insoluble in benzene, chloroform or ether {Kaczka, 1964 #68}. Chemical structure of cordycepin as presented in Figure 3.

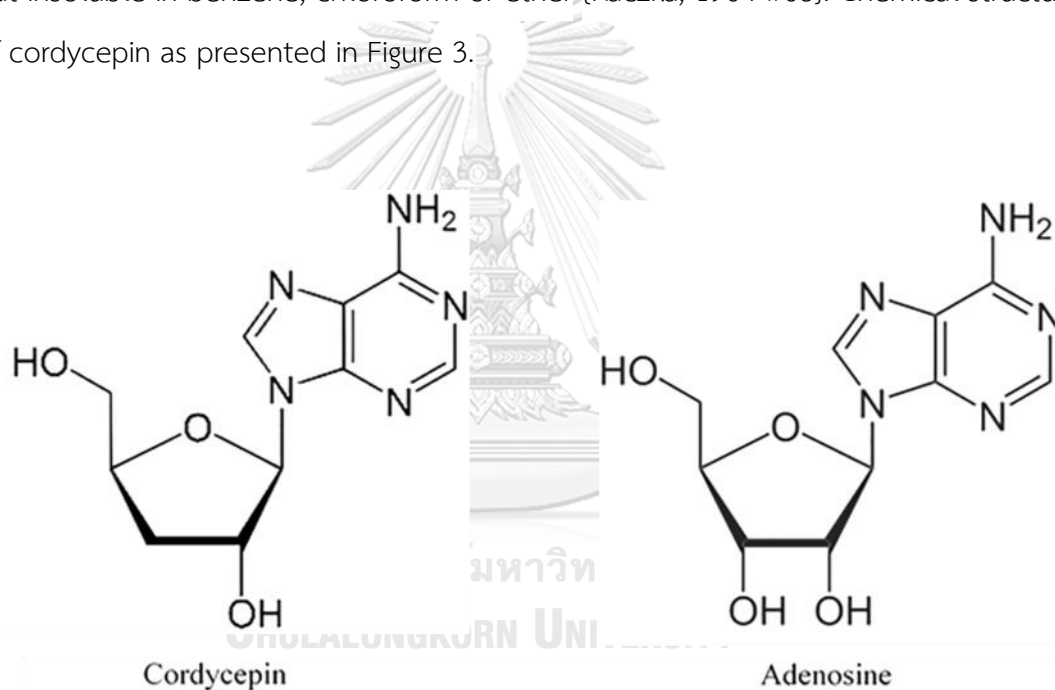


Figure 3 : Chemical structure of cordycepin (3'-deoxyadenosine) and adenosine

II. Classification of Nanoparticles

Based on the basis of their chemical nature, nanoparticles can be broadly categorized into organic and inorganic nanoparticles. (Degli Esposti, Carella et al. 2018) Inorganic nanoparticles are prepared with inorganic materials. Inorganic nanoparticles are being actively exploited for nanotechnology-based biosensors and diagnostics due to their optical and magnetic properties, (Vashist, Venkatesh et al. 2012) such as Gold nanoparticles, silver nanoparticles, magnetic iron oxide, and quantum dots, etc. Organic nanoparticles are prepared from biocompatible and biodegradable biomolecules and biomaterials. The example of organic nanoparticles are dendrimers, micelles, liposomes, ferritin, etc. Organic nanoparticles have been extensively utilized as drug delivery systems due to their well-documented biodegradability and biocompatibility. Of the organic nanoparticles, lipid-based and biodegradable polymeric nanoparticles are the most widely used. Both organic and inorganic nanoparticles are of interest in material and life sciences.

III. Advantages of Nanoparticles.

Nanotechnology-based drug delivery system represents a promising strategy for improving multi-performance characteristics of classical drugs with several improved pharmaceutical actions. To date, various aspects of nanoparticle-mediated drug delivery systems have been well established. Nanoscale drugs are superior to free drugs, as explained by several mechanisms such as encapsulation, selective targeting to diseased sites, sustained, controlled or triggered release, thus improving the pharmacokinetic behavior and target ability of drugs. Encapsulation is defined as “*drug* entrapped within a colloidal system after a formulation process to prevent exposure of the encapsulated drugs to off-target tissues. (Kumari, Singla et al. 2014) This offer a particular advantage for toxic substances such as chemotherapeutic drugs, where off-target toxicity is a main limitation. The controlled release system is referred to as “a constant release of active ingredient that exhibits zero-order kinetics”. (Zhao, Xu et al. 2017) An amount of the drug is continuously released and

equivalent to the eliminated by the body for a specific period of time. Furthermore, drugs can be released in a sustained or triggered manner by choosing appropriate materials and design features. Most interestingly, targeting nanoparticles directly to a certain location in the body (referred to as site specific targeting) is a key success in drug delivery. These systems have potential to reduce off-target effects and enhance accumulation at the diseased tissues or organs.

IV. Methods for construction of nanoparticles

Nanoparticles can be created by several methods, which involve mechanical, chemical and other pathways. (Koczur, Mourdikoudis et al. 2015) Two typical approaches to the construction of organic nanoparticles are “top-down” and “bottom-up” approaches. In the “bottom-up” techniques, nanoparticles are synthesized from small molecules via synthetic chemistry and self-assembly to create a wide range of nanoscale systems such as lipid-based nanoparticles, polymeric nanoparticles, liposomes, and niosomes. In the “top-down” techniques, large particle size of initial materials are broken down by mechanical milling and other more complex ones such as microfluidics and lithography. Small molecule drugs can be loaded into nanoparticles either by conjugation on the surface, or by physical encapsulation.

V. Characterization of nanoparticles

Physicochemical characterization

Particle size (Dynamic Light Scattering, Scanning and Transmission Electron Microscopy, Atomic Force Microscopy)

Physicochemical characterizations of nanoparticles are primarily analyzed by the particle size, charge (Zeta-potential), and morphology. Dynamic light scattering (DLS) offer the frequently used technique for determination of the particle size and size distribution. (de Assis, Mosqueira et al. 2008) In order to visualize the size, shape and surface morphology more accurately, direct observation can be achieved by two

electron microscopy techniques; transmission electron microscopy (TEM) and scanning electron microscopy (SEM). Another microscopy technique known as scanning force microscopy or AFM provides the most accurate description of size, size distribution and actual picture. (Polakovič, Görner et al. 1999)

Surface charge

Surface charge of nanoparticles is an important parameter to evaluate the storage stability. Surface charge determines the electrostatic interaction between nanoparticles as well as their interaction with the biological environment. An indirect measurement of the surface charge is Zeta potential. Either high positive or negative zeta potential values ensure stability and avoid aggregation and precipitation of the nanoparticles. (Otsuka, Nagasaki et al. 2012)

Biological characterization

Cell-based assays

Nanoparticles are biologically characterized for various purposes, namely biological effects, nanotoxicology and interactions between these nanoparticles and their targeted cells ((Nel, Mädler et al. 2009) , (Petros and DeSimone 2010) and (Albanese, Tang et al. 2012)). A wide range of instrumentation have been developed to assess these biological properties in order to avoid large-scale and cost-intensive *in vivo* animal testing(Edmondson, Broglie et al. 2014). If the drugs are exploited for topical delivery, it is possible to use cell-based assays, such as *ex vivo* animal or human skin, and artificial or reconstructed skin models. (Brohem, da Silva Cardeal et al. 2011) Similarly, a wide range of cell-based models (Tan, Trier et al. 2018) and simulated gastrointestinal fluids (Ulleberg, Comi et al. 2011) that mimic the gastrointestinal tract have been developed for testing orally-administered drugs.

Uptake mechanism

The first interaction between nanoparticles and cells is crucial to initiate cell entry. For cellular uptake to occur, nanoparticles must associate with the cell membrane, either through nonspecific (such as electrostatic attraction) or specific (ligand-receptor) binding(Nel, Mädler et al. 2009). Nonspecific binding forces that promote cellular contact and nanoparticle internalization mainly result from intrinsic characteristics of nanoparticles. For example, surface charge (as determined by Zeta

potential value) affects nanoparticles' interactions with charged phospholipid head groups or protein subunits on cell membranes (Fleck and Netz 2004). In addition, characteristics of nanoparticle (for example, size, shape, radius of curvature) also play an important role in their cellular uptake (Chithrani, Ghazani et al. 2006) , (Decuzzi and Ferrari 2007) and (Gao, Shi et al. 2005). In contrast, the specific binding results from interactions between specific ligands and complementary molecules or receptors on the cell membrane, resulting in receptor-mediated endocytosis of nanocarriers (Gao, Shi et al. 2005). Ligands can be either of biological origin (i.e., protein, peptide, antibody or antibody fragment) or abiotic ligands such as chemical moieties or surface functionalities (for example, polymeric substances such as polycationic PEI and polyamidoamine (Leroueil, Berry et al. 2008), all of which initiate binding affinity and subsequent cellular uptake. By exploiting the verity and diversity of cell surface receptors, cellular uptake can be improved by attachment of complementary ligands to nanoparticles.

Many endocytosis pathways have been identified. Large particles can be taken up by phagocytosis. This pathway can be primarily observed in specialised immune cells such as macrophages, dendritic cells, neutrophils, and monocytes. In contrast to phagocytosis, that is found in a few cell types, most cells are capable of macropinocytosis (Oupicky, Ogris et al. 2002). Activation of this pathway leads to intense actin and microfilaments remodelling and membrane ruffling. The other well characterized mechanisms are clathrin-mediated and caveolae-mediated endocytosis. Caveolin-coated vesicles are first delivered to intermediate compartments called caveosomes, whereas clathrin-coated vesicles are directly transported to early endosomes. Nanoparticles are also internalized via a clathrin/caveolin independent entry pathway using clathrin- and dynamin-independent carriers (CLICs) derived from the cell membrane, which subsequently travel to glycosyl phosphatidylinositol-anchored protein enriched early endosomal compartments (GEEC), *en route* to the early endosome.

It is however difficult to determine whether they use multiple entry pathways or different components of one complex pathway. Similarly, the endocytic pathway of previously reported nanoparticles greatly varies with the cell types and molecular component of the cell surface in addition to their intrinsic characteristics (e.g., charge and size, etc.), generating conflicting data regarding the cell uptake mechanism exploited (Marie, Beech et al. 2006) , (Katakura, Harada et al. 2004) and (Wang, Li et al. 2001).



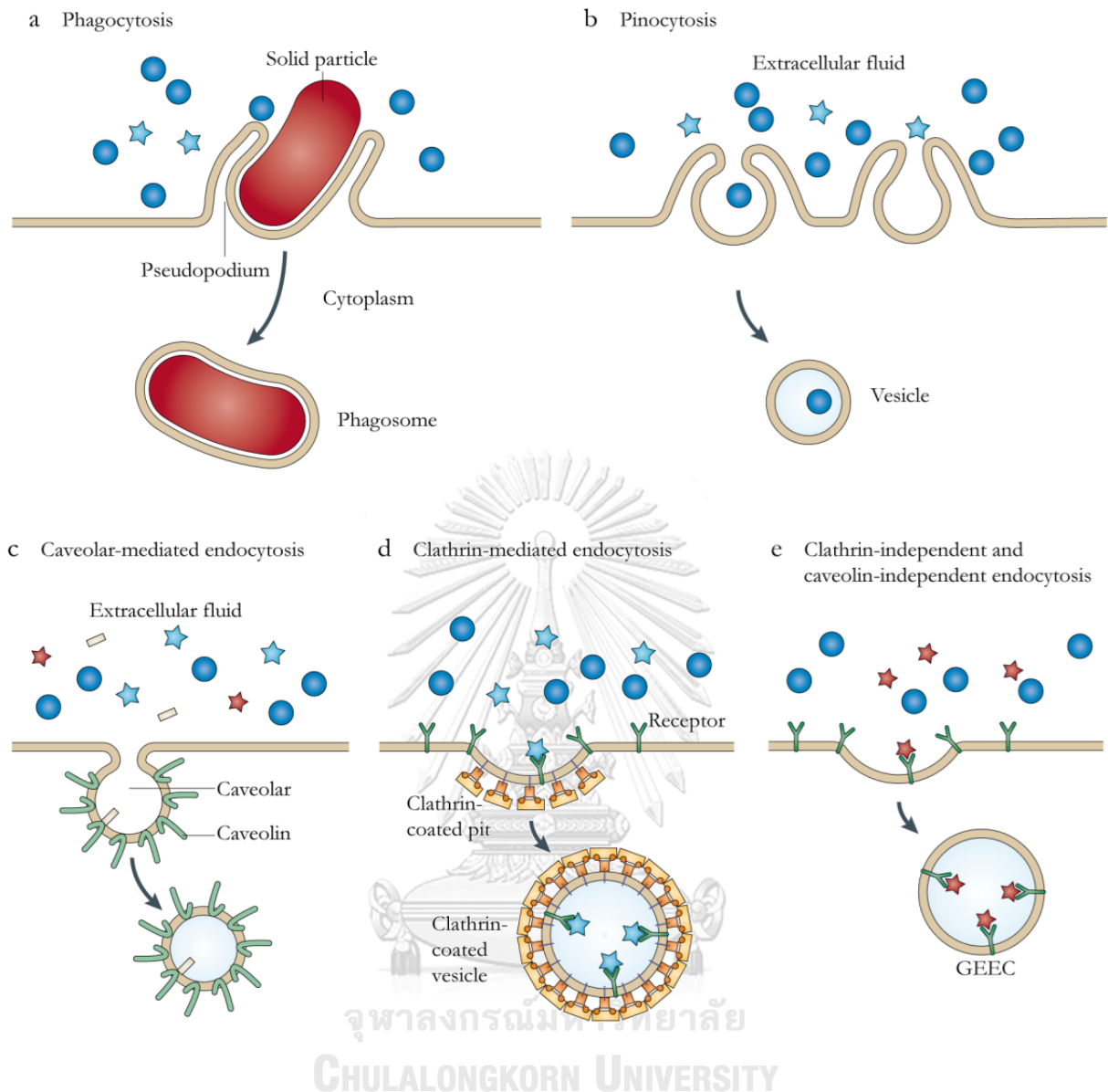


Figure 4 : Pathways of endocytosis. Cellular uptake of large particles is mediated by phagocytosis (a), whereas fluid uptake is facilitated by pinocytosis (b). Different particles can be also internalised through different pathways, including caveolar-mediated endocytosis (c), clathrin-mediated endocytosis (d) and clathrin-independent and caveolin-independent endocytosis (e) (Modified from (Petros and DeSimone 2010))

CHAPTER III

MATERIALS AND METHOD

Materials

Cordycepin, cholesterol, lecithin, sodium cholate hydrate, span80, tween80, chitosan, simulated GI fluids, MTT, DMSO, LIVE/DEAD® Cell Viability/Cytotoxicity Assay Kit, porcine mucin, Tris-base, Deionized water, D-MEM medium, Fetal Bovine Serum (FBS), Penicillin, Streptomycin, L-glutamine, syringe pump, syringe, magnetic stirring, rotary evaporator, Malvern Instruments Zetasizer Nano ZX, sonicator, transwell plate, HPLC, HT29 cell lines, Caco-2 cell lines

Method

Fabrication

1. Preparation of biloniosome nanoparticles

Biloniosomes were prepared by a solvent (ethanol) injection method. Briefly, the aqueous phase was prepared by dissolving the desired amount of cordycepin (20 mg) and polysorbate 80 (100 mg) in 10 ml deionized (DI) water. The prepared aqueous phase was then mixed with 10 ml of solvent phase consisted of lipid components (7 mg of cholesterol and 37 mg of lecithin), sorbitan monooleate (100 mg) and 10 mM sodium cholate hydrate in ethanol. Biloniosomes were spontaneously formed under mechanical stirring at 300 rpm for 10 min. Subsequently, ethanol in the mixture was removed by rotary evaporation under the reduced pressure.

The complexation of biloniosomes with chitosan was performed by adding 1% of small molecular weight (50-200 kDa; Sigma) chitosan, previously dissolved in a solution of 1% acetic acid, into biloniosomes at different ratios from 1:0.5 to 1:5 (v/v) in order to optimize ratios between biloniosome and chitosan solution. The mixture was stirred for 1 hour at room temperature and stored at 4°C until needed for further experiment. The summary of components are presented in Table 1.

Table 1 : Components of biloniosome nanoparticles

HNPs Components	Concentration (mg/ml)
Cordycepin	2
Cholesterol	0.7
Lecithin	3.7
Sodium Cholate Hydrate	4.3
Polysorbate 80	10
Sorbitan monoileate	10
Chitosan 50-200 kDa	5

2. Determination of encapsulation efficiency (EE)

Encapsulation efficiency (EE) of Cordycepin is determined. Briefly, Cordycepin nanoparticles are added onto Amicon membrane filter (Amicon Ultra-15, Merck Millipore Ltd., Darmstadt, Germany). Filled amicon tube are centrifuged at 80,000 rpm for 1 h. Unencapsulated Cordycepin in the aqueous phase (supernatant) is filtered through a 0.22 μm nylon filter and injecting to high performance liquid chromatography (HPLC) (Waters, e2695, Singapore) with Photodiode array detection (PAD) (Waters, 2998 Photodiode Array, Singapore). EE are calculated following Equation:

$$\%EE = \frac{C_i - C_f}{C_i} \times 100$$

Where C_i represents initial concentration of Cordycepin added to biloniosome nanoparticles; C_f represents the concentration of unencapsulated Cordycepin.

3. Physicochemical characterization of biliosome nanoparticles

Dynamic light scattering (DLS) and zeta potential of prepared biliosome nanoparticles are determined using a Malvern Instruments Zetasizer Nano ZX. DLS measurements are carried out using He-Ne laser ($\lambda_0 = 633 \text{ nm}$, $\theta = 173^\circ$). The particle solution is diluted 1,000 times in DI water before measurement. All measurements are performed in triplicate at 25°C.

The particle morphology of biliosome nanoparticles are characterized using transmission electron microscope (JEM-2100 plus, JEOL, Japan) after vacuum-drying. Briefly, the samples are diluted in pure water and dropped directly on copper grid, the samples are observed with magnification of 200.0kX.

4. Stability in gastrointestinal fluids

The experiment was performed to evaluate the physical stability of biliosomes in gastric conditions. The biliosomes were added to the simulated gastric fluid (SGF) comprised 3.2 mg/mL pepsin in 0.2% (w/v) NaCl at pH 1.2, and incubated at 37 °C. The samples of biliosomes were collected at regular intervals and measured the physical properties by using zetasizer. The lipiosome without bile salt was used as control. Dynamic light scattering (DLS) and zeta potential of biliosome nanoparticles are determined using a Malvern Instruments Zetasizer Nano ZX.

5. Cell culture

The human colon carcinoma cell lines (HT29) is maintained in complete D-MEM medium (Thermo Scientific, Massachusetts, USA) supplemented with 10% Fetal Bovine Serum (FBS) (Thermo Scientific), Penicillin (100 units/ml) with Streptomycin (100µg/ml) (Pen & Strep) and L-glutamine (2mM). Cells were grown at 37 °C in a humid atmosphere of 5% CO₂.

The human colon carcinoma cell lines (CaCO-2) is maintained in complete D-MEM medium (Thermo Scientific, Massachusetts, USA) supplemented with 20% Fetal Bovine Serum (FBS) (Thermo Scientific), Penicillin (100 units/ml) with Streptomycin (100µg/ml) (Pen & Strep) and L-glutamine (2mM). Cells were grown at 37 °C in a humid atmosphere of 5% CO₂.

6. Mucoadhesiveness of chitosan-coated biliosomes

To investigate the interaction between mucin and the prepared biliosomes, porcine mucin is dissolved in 10 Mm Tris-base at a concentration of 1% w/v. The mucin solution is stirred at room temperature and centrifuged at 500 rpm for 24 h, followed by sonication (VCX750 probe, Sonics & Materials, Inc., Connecticut, USA) at 40% amplitude for 5 min. The mucin solution is then centrifuged at 25°C 4000 rpm for 20 min to remove the pellet. Chitosan-coated biliosomes or uncoated biliosomes are added to the mucin solution to afford a series of particle:mucin ratios are presented in Table 2. The mixtures are then incubated at 37°C for 1 h, followed by zeta potential and hydrodynamic diameter determination using dynamic light scattering (DLS) (Zetasizer NanoZS, Malvern Instruments, Worcestershire, UK).

Table 2 : A series of particle:mucin ratios (v/v) in mucin mixture

Particle:Mucin ratios (v/v)	Mucin solution	Particle solution	Tris base
1:0.6	300 µl	500 µl	200 µl
1:0.75	300 µl	400 µl	300 µl
1:1	300 µl	300 µl	400 µl
1:1.5	300 µl	200 µl	500 µl
1:3	300 µl	100 µl	600 µl

7. In vitro model of the human intestinal follicle-associated epithelium

The human intestinal epithelial cell line (Caco-2) cultivation is established on the apical chamber of a Corning® 12-well plate Transwell inserts (polycarbonate membrane, polystyrene plate, 0.4 μm pore size, 12 mm diameter, Corning®, New York, NY, USA) in complete DMEM medium. Cells were allowed to differentiate for 21 days with regular medium changes. Transepithelial electrical resistance (TEER) measurement was also used to assess the formation of a cell monolayer with maintenance of tight junction integrity. Only wells with TEER values of at least 0.3 $\text{k}\Omega/\text{cm}^2$ were used in permeation experiments. Free Cordycepin and different formulations of Cordycepin-loaded biliosomes are introduced into the apical chamber of transwells as presented in Figure 5. The basolateral solution was collected after 30 min, 1 h, 3 h and 6 h incubation. The presence of Cordycepin in the basolateral chamber is quantified by HPLC-UV technique. All data and statistical analysis were performed using the GraphPad InStat 3 software (GraphPad Software, Inc., California, USA).

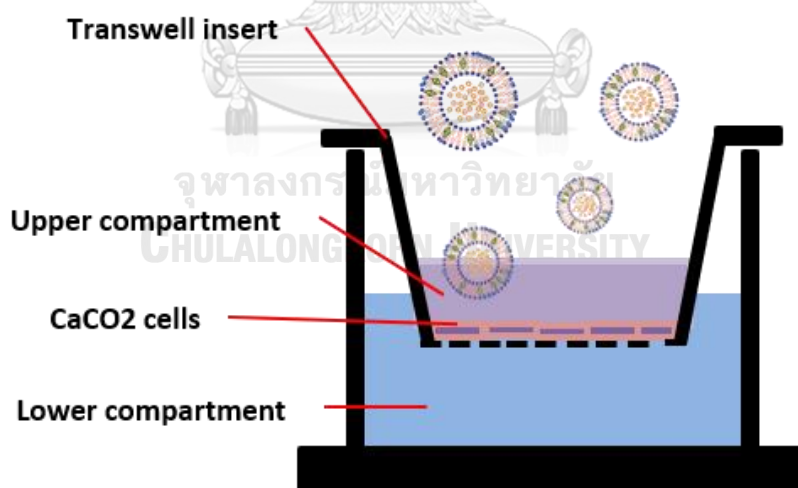


Figure 5 : Caco-2 cultivation is established on the apical chamber of a Corning® 12-well plate Transwell inserts (polycarbonate membrane, polystyrene plate, 0.4 μm pore size, 12 mm diameter, Corning®, New York, NY, USA).

8. Cell viability

Cell viability is evaluated by The *MTT* (3-(4,5-dimethylthiazol-2-yl)-2,5-diphenyltetrazolium bromide) tetrazolium reduction assay which is a colorimetric assay that measures the reduction of yellow 3-(4,5-dimethylthiazol-2-yl)-2,5-diphenyl tetrazolium bromide (MTT) by mitochondrial succinate dehydrogenase. Colorectal cancer cells are seeded at a density of 1×10^4 cells/well in 96-well plates and allowed to grow until 70-80% confluent followed by treatment with Cordycepin-loaded bilosomes. Cytotoxicity was examined 24 h post incubation by adding 100ul MTT solution (1 mg/1 ml of PBS) to each well followed by incubation for 4 h at 37°C. MTT solution is removed and the formazan crystals are dissolved by adding 100ul DMSO to each well. Finally, the absorbance is measured at 570 nm. % Cell Viability is calculated according to the following formula:

$$\% \text{ cell viability} = \frac{\text{OD}_{\text{test}} - \text{OD}_{\text{blank}}}{\text{OD}_{\text{control}} - \text{OD}_{\text{blank}}} \times 100$$

9. Tumor spheroids

In order to obtain spheroids, The human colon carcinoma cell lines (HT-29) were seeded and grown in ultra-low attachment 96-well round-bottomed plates. After 5 days, cells were photographed by light microscope, followed by treatment with nanoparticles for 48 hr. Cell viability was measured by luminescent cell viability assay (CellTiter-Glo, Promega, Madison, WI, USA) based on quantitation of the ATP, which represents number of viable cells. Briefly, tumor spheroids were incubated with lysis buffer for 20 min, then the supernatant were collected and mix with reagents for approximately 10 min at room temperature in opaque well plate. The luminometer (SpectraMax L microplate reader, San Jose, CA, USA) was used for recording the data.

Cells are also stained with the reagents in the LIVE/DEAD® Cell Viability/Cytotoxicity Assay Kit (Invitrogen). Caspases 3/7 activity and Annexin V-FITC/*propidium iodide* (PI) staining as indicator of apoptosis/necrosis are examined according to the manufacturer's instructions.

10. Gene expression analysis

Cells were treated with PBS, cordycepin, chitosan-bilniosome, or chitosan-bilniosome encapsulated cordycepin for 6 hours at 120 ppm. The mRNA levels of BCL2-associated X protein (BAX), B-cell CLL/lymphoma 2 (BCL2), BCL-XL (BCL2L1), human cyclin D1 (CCND1), and cyclin-dependent kinase 4 (CDK4) genes in HT-29 cells were analyzed by RT-qPCR. Total RNA was extracted using the RNeasy mini kit (QIAGEN, Hilden, Germany) and quantified using a NanoDrop spectrophotometer (Thermo Scientific). 1.5 µg of total RNA was treated with RNase-free DNaseI and converted to cDNA using the Maxima First Strand cDNA Synthesis Kit for RT-qPCR with dsDNase (Thermo Scientific). The synthesized cDNA was used as a template for qPCR, performed on a Biorad CFX96 Touch (Bio-Rad, California, USA) instrument using SsoAdvanced™ Universal SYBR® Green Supermix (Bio-Rad). Amplification and detection were performed according to the manufacturer's protocol, followed by melting curve analysis starting at 65°C with increments of 0.5°C per cycle. The primers and annealing temperatures (Ta) used were as follows: CCND1 (60.0°C), FWD (5'-CCTCGGTGTCCTACTTCAAATGTG-3') and REV (5'-GTTCCCTCGCAGACCTCCAGC-3'); CDK4 (60.0°C), FWD (5'-GGACATATCTGGACAAGGCACC-3') and REV (5'-ACTGTTCCACCACTTGTCCAG-3'); BCL2 (60.0°C), FWD (5'-CGACTTCGCCGAGATGTCC-3') and REV (5'-CACACATGACCCACCGAAC-3'); BCL-XL (60.0°C), FWD (5'-CACTGTGCGTGAAAGCGT-3') and REV (5'-CTCTAGGTGGTCATTTCAGGTAAGTG-3'); BAX (60.0°C), FWD (5'-CAGGATGCGTCCACCAAGAAG-3') and REV (5'-AAAACATGTCAGCTGCCACTCG-3'). Expression level was normalized internally to that of control GAPDH (62.5°C): FWD (5'-GGGAACTGTGGCGTGATGG-3') and REV (5'-TGGAGGAGTGGGTGTCGCTG-3') and RPS13 (60.0°C) (assay ID: qHsaCID0038672, Bio-Rad) using the $\Delta\Delta C_t$ method. Assays were performed in triplicate and data were analyzed by the Bio-Rad CFX manager software.

CHAPTER IV

RESULTS AND DISCUSSIONS

In this study, we report the preparation and physicochemical properties of novel biliosome nanoparticles which are based on the bile salt-niosome hybrid system. In addition, we demonstrate the improved properties of nanoparticle, both the stability in the gastrointestinal tract and the therapeutic efficacy of Cordycepin.

1. Characterizations of biliosome nanoparticle

Biliosome nanoparticles were synthesized by a solvent injection method. In this method, the nanoparticles were synthesized from small molecule of lipid and surfactants via self-assembly to form a wide range of nanoscale systems. Small molecule of cordycepin was loaded into the nanoparticles by physical encapsulation. In the present study, the encapsulation efficiency of cordycepin in Biliosome nanoparticles was 82.26%.

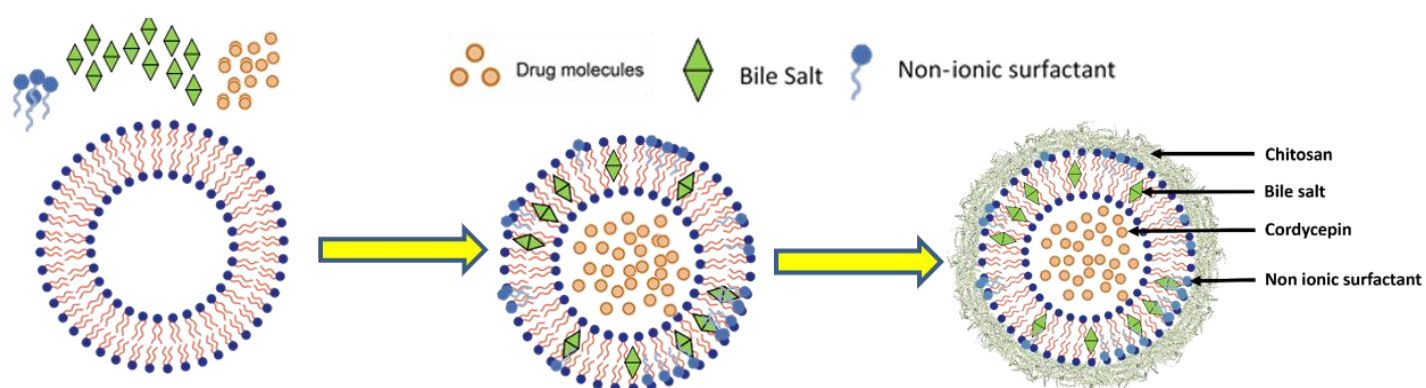


Figure 6 : Schematic diagram of the chitosan-complexed biliosome. The negatively charged biliosome were electrostatically with cationic chitosan polymers to form chitosan- biliosome complexes.

To observe the physicochemical properties of the biliosome nanoparticles, we investigated their size characteristics by measuring average diameter and ζ -potential. The results showed that the hydrodynamic diameter and ζ -potential of cordycepin encapsulated nanoparticles were 227.933 ± 13.4 nm and -31.83 ± 0.6 mV, respectively. The surface charge of the nanoparticles was characterized and found to be negatively charge due to the presence of fatty acids and bile salt, which is normally observed in lipid carriers. Moreover, characteristics of the biliosome nanoparticles were confirmed by TEM as well. The image supported the size diameter results obtained by the DLS. As shown in Figure 7, it showed the spherical shape nanoparticles which a high electron density core, as expected for lipid nano-encapsulation, was located in the center of the nanoparticle.

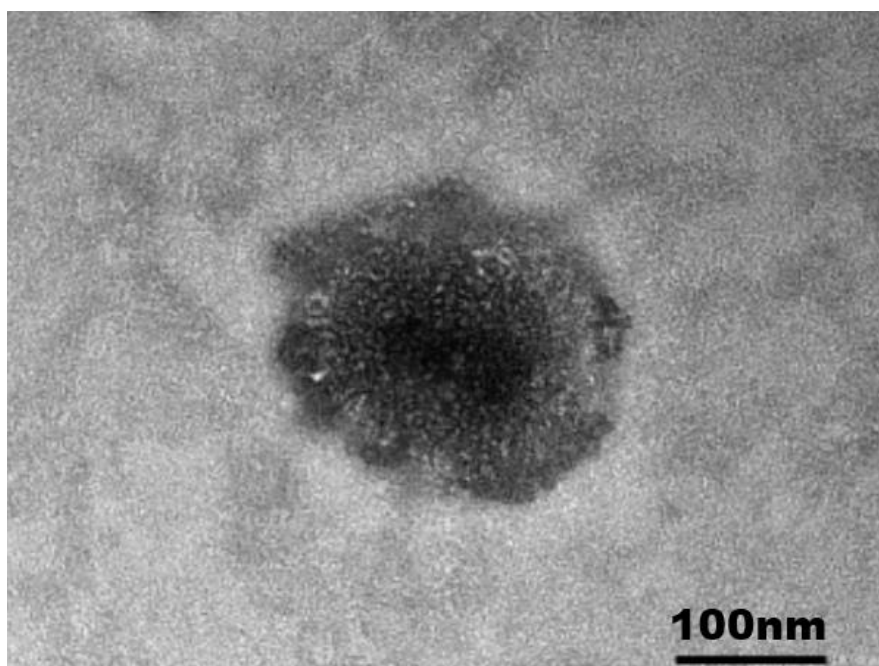


Figure 7 : TEM images of chitosan complexed biliosome

Subsequent experiments were performed to modify the surface charge of nanoparticle in order to improve mucoadhesive properties by chitosan coating. The surface charge and aggregation of nanoparticles depends on the amount of chitosan incorporated on their surface through electrostatic interactions. Different ratios of nanoparticle/chitosan were found to have a significant effect on the ζ -potential values as presented in Figure 8. The original ζ -potential value of biliosome nanoparticles were negatively charge, and then the addition of chitosan into the system caused drastically increase of ζ -potential value to positively charge. The rapid increase in ζ -potential value over this range indicated the drop in hydrodynamic diameter is due to electrostatic repulsion between positive nanoparticles. Interestingly, shifting the nanoparticle/chitosan ratio from 1:0.2 to 1:0.5 resulted in significant increase in ζ -potential value and decrease in hydrodynamic diameter of nanoparticles as same as the original size. However, for low ratios (1:0.5 and below) zeta potential appear to plateau which may be a consequence of chitosan saturation on the nanoparticle surface. Based on the results, optimum concentration of nanoparticle/chitosan (1:0.5) was determined for further studies.

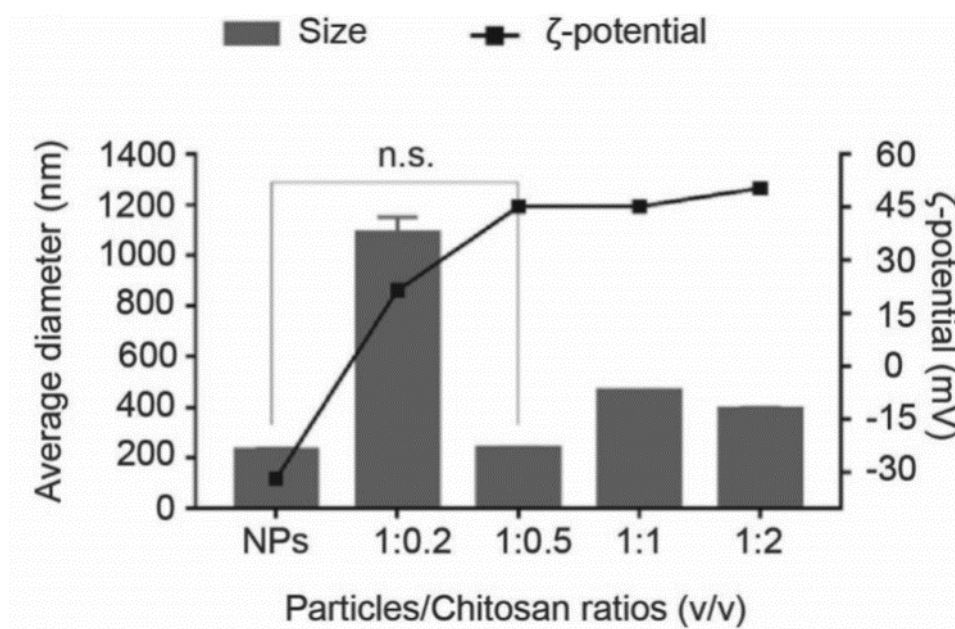


Figure 8 : The optimization of the ratio between chitosan and biliosome (v/v) by using size and zeta potential. (size; n.s. $p \geq 0.001$; one-way ANOVA with Tukey post test)

2. Gastric stability

We believed that the bile salt incorporated nanoparticles can improve the stability of prepared biliosome nanoparticles in gastric conditions. Hence we carried out an experiment to demonstrate their endurance in harsh gastric tract containing pepsin in pH 1.2. Their stability was observed directly from their hydrodynamic sizes over 60 min period. As illustrated in Figure 9, cholate nanoparticle was stable in particle size and size distribution throughout incubation in gastric fluid. On the other hand, the particle size and Percentage Difference Index of plain nanoparticle were unreliability increased during incubation time. This results showed that the bile salt incorporated in nanoparticles makes their membrane flexible which accounts for their rupture under acidic environment (Gupta, Mishra et al. 2005, Chen, Lu et al. 2009). Moreover, nanoparticles containing bile salt can inhibit protease activity and significantly contributes to the reduction of protein degradation, as pepsin cannot diffuse through the nanoparticle membranes, which shields encapsulated protein from enzymatic degradation (Yamamoto, Taniguchi et al. 1994).

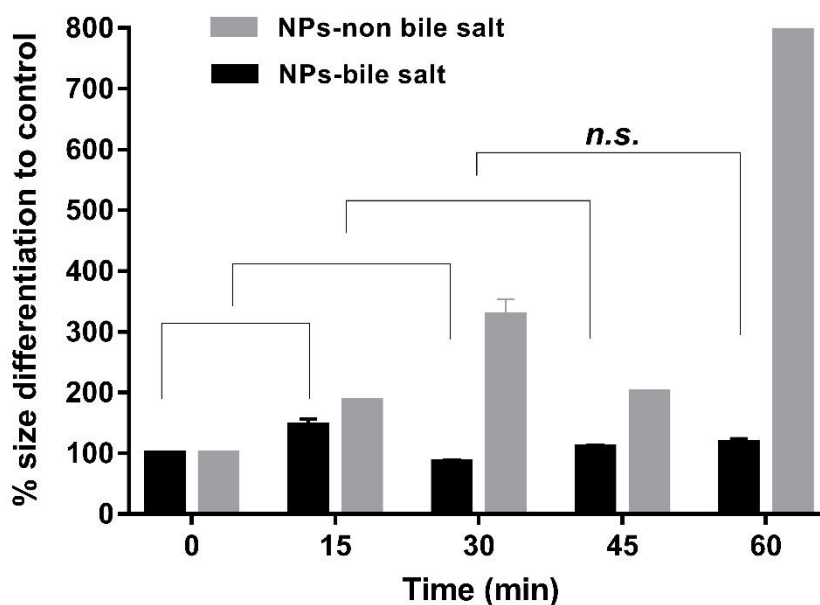


Figure 9 In vitro gastric stability assay of nanoparticles in simulated gastric fluid (SGF) comprising pepsin at pH 1.2 and incubated at 37 °C for 1 hr. Data represents mean \pm SEM from 3 independent measurements (n=3).

3. Mucoadhesive properties

The mucoadhesion interaction of nanoparticles were explored via in vitro mucin assay by precisely measuring their hydrodynamic sizes and ζ -potential values which depends on amount of mucin in the mixture. According to Figure 10, the ζ -potential value of chitosan coated biloniosome were positively charged as reported in previous studies (Lee, Kim et al. 2011, Kozhikhova, Ivantsova et al. 2018). When introduced mucin into the system, the surface charge of nanoparticles were decrease radically from positively charge to negatively charge. The mucin presents negative charge due to the presence of oligosaccharide chains containing carboxyl and sulphate groups. When the mucin was added to the nanoparticles, decrease of positively charge was observed compared to non-chitosan coated biloniosome (steady negative charge).

Likewise, hydrodynamics sizes of nanoparticles were also assessed. The results revealed that chitosan coated biloniosomes were 2-3 folds larger than original size in mucin mixture due to electrostatic repulsion between nanoparticles, but not in non-chitosan coated biloniosome. It indicates that the addition of mucin created an interference with the nanoparticles size distribution which aggregate the system, confirm that mucoadhesion has occurred (Pekker and Shneider 2014). Thus, the chitosan coated biloniosomes have potential for used as a novel oral administered system instead of conventional system because of their stability in gastric tract and their mucoadhesion to mucosal membrane in GI tract.

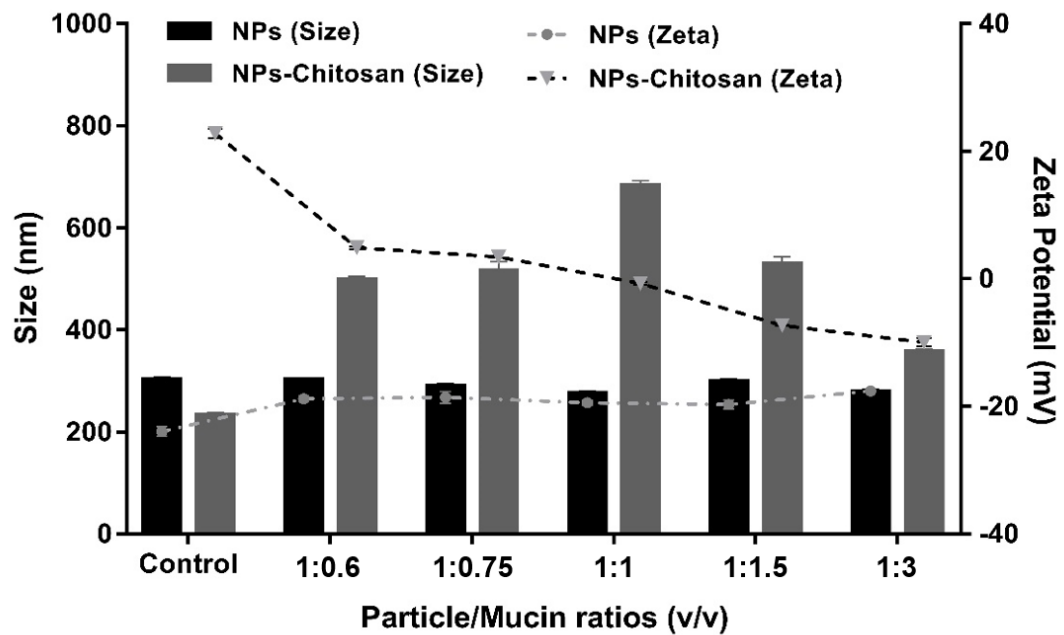


Figure 10 : *In vitro* mucoadhesive assay between biliosome nanoparticles and purified porcine intestinal mucin. The adhesive properties were observed by the differentiation of size and zeta potential of nanoparticle in mucin mixtures incubated at 37°C for 1 hr. (n.s. $p \geq 0.001$; one-way ANOVA with Tukey post test). Data represents mean \pm SEM from 3 independent measurements (n=3).

4. Permeability assay

To measure the intestinal absorption of cordycepin biliosome, human colon epithelial cell line (Caco-2) was employed as a model for human intestinal epithelium. Caco-2 cells were cultured (21 days) and Transepithelial electrical resistance (TEER) value are from 1800 to 2200 $\Omega \cdot \text{cm}^2$. The transported amount of cordycepin was plotted as a function of time versus percent of permeability directly calculated from amount of cordycepin across model to lower chamber over period of time. Based on the results shown in Figure 12, chitosan coated nanoparticles significantly increased permeability of cordycepin through the model compared to non-coated nanoparticle and free cordycepin. These results may be explained by the increasing of ζ -potential values that occurs on the surface of chitosan coated nanoparticles. Therefore, cellular membranes presented negatively charge are more attracting to positively charge nanoparticles and leading to increased paracellular transport of nanoparticles (Yue, Wei et al. 2011, Alqahtani, Simon et al. 2015). Thus, it can conclude that the positive charge of chitosan led to increased uptake efficiency of nanoparticles and increase permeability of cordycepin as well

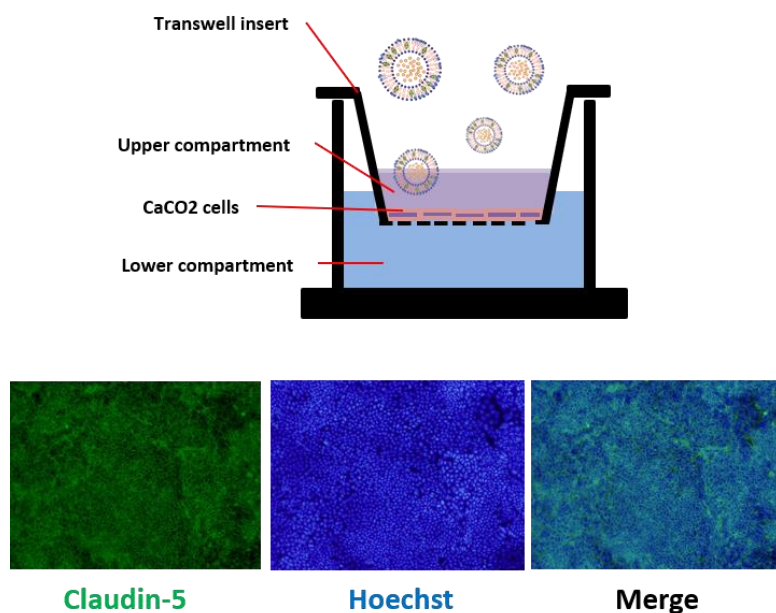


Figure 11 : Caco2 cultured transwell assay was established to evaluate the transcytosis of biliosome nanoparticles. 2 cultured transwell permeability assay for biliosome nanoparticles. The expression of tight junction protein claudin-5. Green: claudin-5 proteins; Blue: Hoechst, cell nucleus.

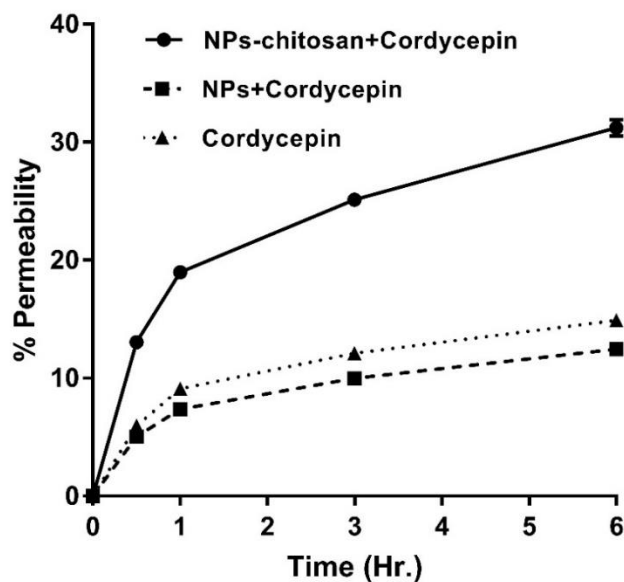


Figure 12 : The permeability of nanoparticles were directly evaluated with amount of cordycepin through transwells by HPLC, compared to cordycepin, at 37°C. The solution was collected in bottom wells after 30 min, 1 h, 3 h and 6 h incubation. Data represents mean \pm SEM from 4 independent measurements (n=4).

5. Anti-cancer and gene expression analysis

The therapeutic potential of cordycepin has been well known for its wide range of applications which was reported in many studies (Tuli, Sharma et al. 2013, Tuli, Sandhu et al. 2014), especially, anticancer therapeutics (Lee, Hong et al. 2011). In our experiment, we elucidated a promising strategy of nanoparticles for improving characteristics of cordycepin with enhanced pharmaceutical actions. The effect of cordycepin and cordycepin encapsulated biloniosome in suppressing the proliferation of colorectal cancer cell (HT-29) were determined after 48 h treatment of various concentrations. HT-29 cells presented dose-dependent decline in cell viability (Figure 13, suggesting cordycepin suppress cancer cell proliferation. Notably, significant improvement in cancer cell suppression appeared from the cordycepin encapsulated nanoparticle and free cordycepin at the same concentration.

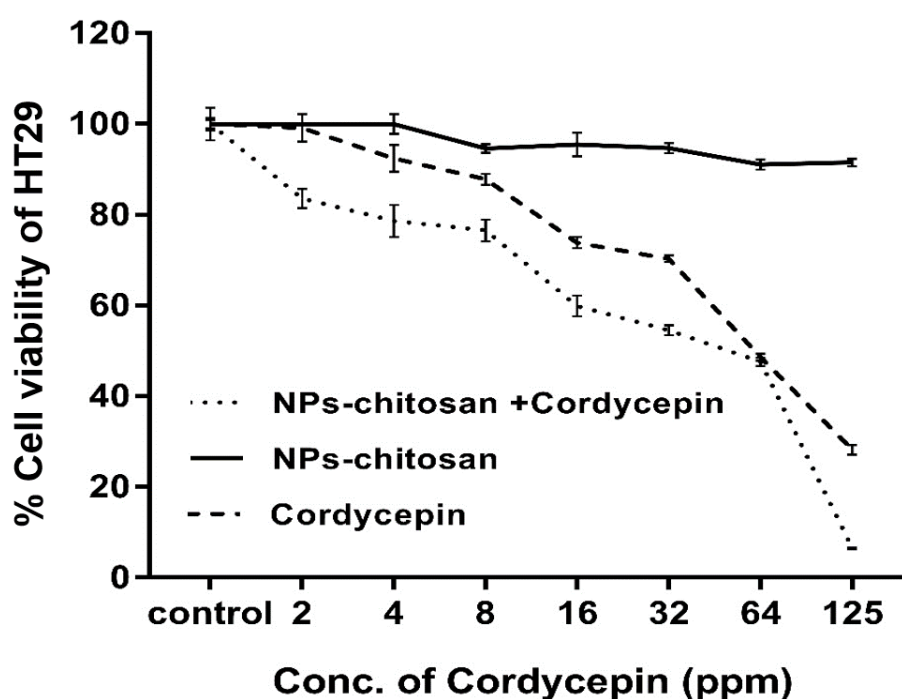


Figure 13 : Effects of cordycepin and biloniosome nanoparticles encapsulated cordycepin on colorectal cancer cell (HT-29). % cell viability. HT-29 cell were treated with nanoparticles for 24 hr. and determined by MTT assay. Data represents mean \pm SEM from 8 independent measurements ($n=8$).

In addition, expressions of genes regulating cell proliferation (CCND1 and CDK4) and apoptosis (BCL-2, BCL-XL, and Bax) were investigated in a human colorectal adenocarcinoma cell (HT-29) for evaluation of apoptotic mechanism. Cells were treated for 6 h with 120 ppm of cordycepin, cordycepin encapsulated biloniosome, or control (1XPBS or plain biloniosome). The transcript levels of target genes were quantified by RT-qPCR. GAPDH and RPS13 were selected as reference genes for data normalization due to their stable expression across the experimental conditions, giving CV = 0.0624 and M = 0.1801 [for homogenous (CV < 0.25; M < 0.5), heterogeneous (CV < 0.5; M < 1)]. Figure 14 and 15 showed that treatment of HT-29 cells with 120 ppm of either pure cordycepin or biloniosome-encapsulated cordycepin led to significant downregulation of anti-apoptotic gene BCL-XL transcript without affecting expression levels of CCND1, CDK4, BCL-2, and BAX. It is noteworthy that we did not observe cordycepin-induced Bax expression in HT-29 cells as previously documented by Lee SY et al. (Lee, Debnath et al. 2013). The discrepancy might be due to differences in an incubation time used in the experiments (6 h vs 18 h) as well as the assayed biomolecules (mRNA vs protein). However, there is no significant difference in expression between treated with cordycepin alone and the group treated with cordycepin encapsulated biloniosome. Therefore, we conclude that cordycepin and biloniosome-encapsulated cordycepin can induce apoptosis in cancer cell (same manner) by negatively regulating an expression of BCL-XL.

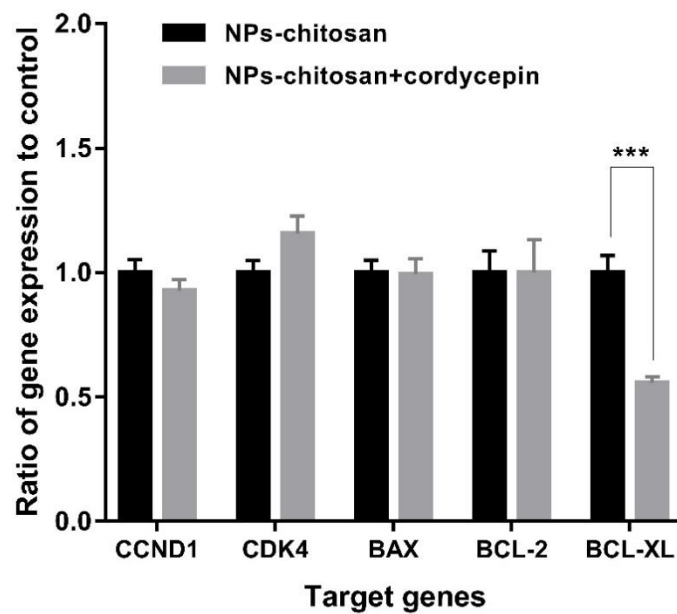
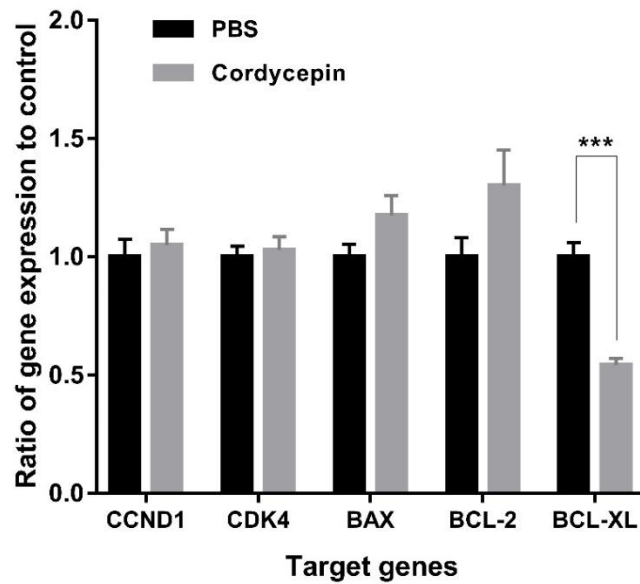


Figure 14, 15 : Cell transcript expression levels of genes regulating cell proliferation and apoptosis. HT-29 cells were untreated or treated for 6 h with 120 $\mu\text{g/ml}$ of (12.) cordycepin or (13.) nanoparticles-encapsulated cordycepin. Total RNA was extracted, DNase-treated, and converted to cDNA. Relative expression levels of CCND1, CDK4, BCL2, BCL-XL, and BAX genes were analyzed by RT-qPCR. Data were normalized to the GAPDH and RPS13 levels present in the same samples. (***) $p < 0.001$; one-way ANOVA with Tukey post test).

Next, we determined the effects of cordycepin encapsulated nanoparticles in 3D spheroid model of colorectal cancer cell, which mimic the tumor organization. They are considered as reliable models than conventional cultures in 2D culture. HT-29 cells were cultured in ultra-low attachment plate for 5 days followed by treatment with cordycepin encapsulated nanoparticles for 48 hr of various concentrations. Then, spheroids were stained by using live/dead cell viability dye (Figures 16). Significant dead cells (red) in spheroid was observed on cordycepin nanoparticle treated compared to cordycepin alone treatment, which is correlated to cell availability in Figure 17. Cell viability of spheroid was continuously decreased with dose-dependent manner, especially at 100 ppm, statistically significant cell death as observed in cordycepin-nanoparticles. However, free cordycepin radically induce cell proliferation at low concentration (5 ppm and 100 ppm), which was not noticed in 2D culture model. Ju-Hyon Lee et.al. (Lee, Hong et al. 2011), reported that cordycepin presented effective anti-cancer activity via direct cellular apoptotic effect, but cordycepin treatment failed to inhibit complexed tumor model at low concentrations (Lee, Hong et al. 2011). Accordingly, the formulation of cordycepin biliosome in the optimal dose of cordycepin can reduced tumor spheroid more efficient than free cordycepin.

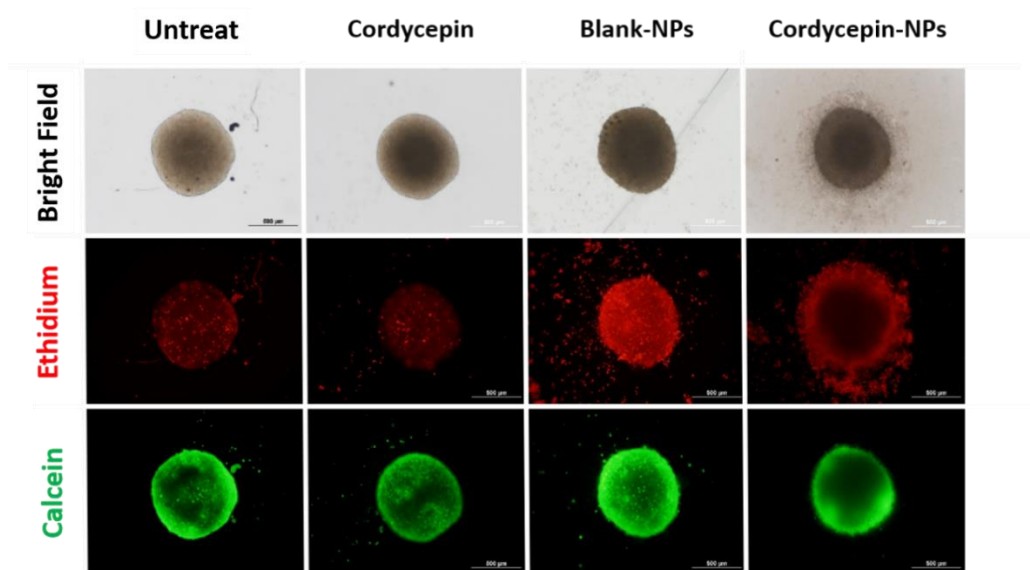


Figure 16 : Tumor spheroids were stained by live/dead cell viability dye; dead cells (red-ethidium homodimer-1), live cells (green-Calcein, AM)

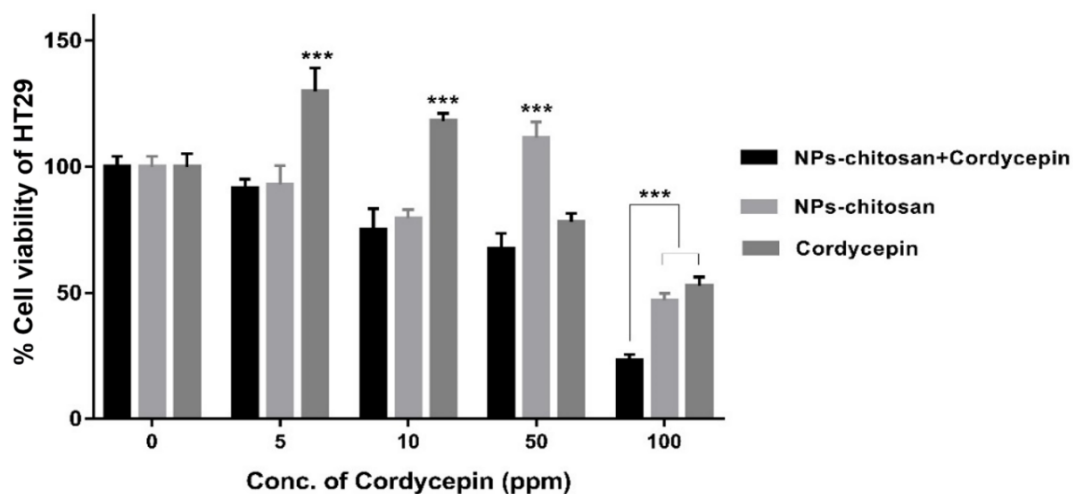


Figure 17 : 3D spheroid assay model of colorectal cancer cell (HT-29). HT-29 cell were seeded and grown in ultra-low attachment round-bottomed plates, after 5 days, then treated with cordycepin encapsulated nanoparticles at 100 ppm for 48 hr. % cell availability were measured by luminescent cell viability assay. Data represents mean \pm SEM from 4 independent measurements ($n=4$). (***) $p < 0.001$; one-way ANOVA with Tukey post test).

The results showed that the nanoparticles can associate with the cell membrane, either through nonspecific (such as electrostatic attraction) (Nel, Mädler et al. 2009) or receptor-mediated endocytosis of nanoparticles. Firstly, nonspecific binding forces that promote cellular contact and nanoparticle internalization mainly result from intrinsic characteristics of nanoparticles. For example, surface charge (as determined by ζ -potential value) affects nanoparticle interactions with charged phospholipid head groups or protein subunits on cell membranes (Fleck and Netz 2004). Then, nanoparticles receptor-mediated protein on cellular membrane play significant role in endocytosis. Activation of this pathway leads to intense actin and microfilaments remodeling and membrane ruffling by the well characterized mechanisms viz., clathrin-mediated and caveolae-mediated endocytosis (Petros and DeSimone 2010). Thus, it is recommended that biliosome nanoparticles are novel and practical application to enhance anti-cancer proliferating activities of cordycepin.

CHAPTER V

CONCLUSIONS

In this study, we have developed and successfully evaluated an improved formulation of the biliosome-core/chitosan-shell hybrid nanoparticles. Our study have demonstrated the in vitro performance of this hybrid system to enhance the efficacy of orally administered Cordycepin. To achieve this goal, three specific strategies are combined. Firstly, niosomes formed by self-association of nonionic surfactants lipid and cholesterol were exploited as a vesicle-based nanocarrier system for efficient delivery of Cordycepins. Secondly, the incorporation of bile salts into nanoparticles was to circumvent the issue of nanoparticle degradation in the gastrointestinal tract. Thirdly, surface modification with mucoadhesive chitosan biopolymer was also exploited to circumvent the issue of inefficient targeting nanoparticles to mucosal surfaces. Through monitoring stability in gastric condition, mucoadhesive properties, and permeability across intestinal epithelium model, and cancerous therapeutics effect, the hybrid nanoparticles were retained significantly superior in comparison with conventional system, particularly, the stability and therapeutic efficacy of Cordycepin. These results provide a promising potential oral application not only for cordycepin itself but also for other pharmaceutical molecules as an oral medicine or alternative to chemotherapy in gastrointestinal cancer treatments.

REFERENCES

Aburahma, M. H. (2016). "Bile salts-containing vesicles: promising pharmaceutical carriers for oral delivery of poorly water-soluble drugs and peptide/protein-based therapeutics or vaccines." Drug delivery **23**(6): 1847-1867.

Ag Seleci, D., et al. (2016). "Niosomes as nanoparticulate drug carriers: fundamentals and recent applications." Journal of nanomaterials **2016**.

Albanese, A., et al. (2012). "The effect of nanoparticle size, shape, and surface chemistry on biological systems." Annual review of biomedical engineering **14**: 1-16.

Alqahtani, S., et al. (2015). "Cellular uptake, antioxidant and antiproliferative activity of entrapped α -tocopherol and γ -tocotrienol in poly (lactic-co-glycolic) acid (PLGA) and chitosan covered PLGA nanoparticles (PLGA-Chi)." Journal of colloid and interface science **445**: 243-251.

Bernkop-Schnürch, A. (2013). "Reprint of: Nanocarrier systems for oral drug delivery: Do we really need them?" European Journal of Pharmaceutical Sciences **50**(1): 2-7.

Brohem, C. A., et al. (2011). "Artificial skin in perspective: concepts and applications." Pigment cell & melanoma research **24**(1): 35-50.

Buenz, E., et al. (2005). "The traditional Chinese medicine Cordyceps sinensis and its effects on apoptotic homeostasis." Journal of ethnopharmacology **96**(1-2): 19-29.

Chen, Y., et al. (2009). "Enhanced bioavailability of the poorly water-soluble drug fenofibrate by using liposomes containing a bile salt." International Journal of

Pharmaceutics **376**(1-2): 153-160.

Cheung, R. C. F., et al. (2015). "Chitosan: an update on potential biomedical and pharmaceutical applications." Marine drugs **13**(8): 5156-5186.

Chithrani, B. D., et al. (2006). "Determining the size and shape dependence of gold nanoparticle uptake into mammalian cells." Nano Letters **6**(4): 662-668.

Cunningham, K., et al. (1950). "Cordycepin, a metabolic product isolated from cultures of *Cordyceps militaris* (Linn.) Link." Nature **166**(4231): 949-949.

de Assis, D. N., et al. (2008). "Release profiles and morphological characterization by atomic force microscopy and photon correlation spectroscopy of ^{99m}Techetium-fluconazole nanocapsules." International Journal of Pharmaceutics **349**(1-2): 152-160.

Decuzzi, P. and M. Ferrari (2007). "The role of specific and non-specific interactions in receptor-mediated endocytosis of nanoparticles." Biomaterials **28**(18): 2915-2922.

Degli Esposti, L., et al. (2018). Inorganic nanoparticles for theranostic use. Electrofluidodynamic Technologies (EFDTs) for Biomaterials and Medical Devices, Elsevier: 351-376.

Edmondson, R., et al. (2014). "Three-dimensional cell culture systems and their applications in drug discovery and cell-based biosensors." Assay and drug development technologies **12**(4): 207-218.

Fleck, C. C. and R. Netz (2004). "Electrostatic colloid-membrane binding." EPL

(Europhysics Letters) **67**(2): 314.

Fricker, G., et al. (2010). "Phospholipids and lipid-based formulations in oral drug delivery." Pharmaceutical research **27**(8): 1469-1486.

Gao, H., et al. (2005). "Mechanics of receptor-mediated endocytosis." Proceedings of the National Academy of Sciences **102**(27): 9469-9474.

Gong, H., et al. (2000). "Effects of Cordyceps sinensis on T lymphocyte subsets and hepatofibrosis in patients with chronic hepatitis B." Hunan yi ke da xue xue bao= Hunan yike daxue xuebao= Bulletin of Hunan Medical University **25**(3): 248-250.

Gupta, P. N., et al. (2005). "Non-invasive vaccine delivery in transfersomes, niosomes and liposomes: a comparative study." International Journal of Pharmaceutics **293**(1-2): 73-82.

Hur, H. (2008). "Chemical ingredients of Cordyceps militaris." Mycobiology **36**(4): 233-235.

Kaczka, E. A., et al. (1964). "Identification of cordycepin, a metabolite of Cordyceps militaris, as 3'-deoxyadenosine." Biochemical and biophysical research communications **14**: 456-457.

Katakura, H., et al. (2004). "Improvement of retroviral vectors by coating with poly (ethylene glycol)-poly (L-lysine) block copolymer (PEG-PLL)." The Journal of Gene Medicine: A cross-disciplinary journal for research on the science of gene transfer and its clinical applications **6**(4): 471-477.

KIHO, T., et al. (1993). "Polysaccharides in fungi. XXXII. Hypoglycemic activity and chemical properties of a polysaccharide from the cultural mycelium of *Cordyceps sinensis*." Biological and Pharmaceutical Bulletin **16**(12): 1291-1293.

Kiho, T., et al. (1999). "Structural features and hypoglycemic activity of a polysaccharide (CS-F10) from the cultured mycelium of *Cordyceps sinensis*." Biological and Pharmaceutical Bulletin **22**(9): 966-970.

Koczkur, K. M., et al. (2015). "Polyvinylpyrrolidone (PVP) in nanoparticle synthesis." Dalton Transactions **44**(41): 17883-17905.

Koh, J.-H., et al. (2003). "Hypocholesterolemic effect of hot-water extract from mycelia of *Cordyceps sinensis*." Biological and Pharmaceutical Bulletin **26**(1): 84-87.

Kozhikhova, K. V., et al. (2018). "Preparation of chitosan-coated liposomes as a novel carrier system for the antiviral drug Triazavirin." Pharmaceutical development and technology **23**(4): 334-342.

Kumari, A., et al. (2014). "Nanoencapsulation for drug delivery." EXCLI journal **13**: 265.

Lee, C.-M., et al. (2011). "Effects of Chitosan Coating for Liposomes as an Oral Carrier."

대한의생명과학회지 **17**(3): 211-216.

Lee, J.-H., et al. (2011). "Anti-cancer effects of cordycepin on oral squamous cell carcinoma proliferation and apoptosis in vitro." J Cancer Ther **2**(02): 224.

Lee, J. B., et al. (2017). "Development of cordycepin formulations for preclinical and clinical studies." Aaps Pharmscitech **18**(8): 3219-3226.

Lee, S. Y., et al. (2013). "Anti-cancer effect and apoptosis induction of cordycepin through DR3 pathway in the human colonic cancer cell HT-29." Food and chemical toxicology **60**: 439-447.

Lennon, M. B. and R. J. Suhadolnik (1976). "Biosynthesis of 3'-deoxyadenosine by *Cordyceps militaris*: mechanism of reduction." Biochimica et Biophysica Acta (BBA)-Nucleic Acids and Protein Synthesis **425**(4): 532-536.

Leroueil, P. R., et al. (2008). "Wide varieties of cationic nanoparticles induce defects in supported lipid bilayers." Nano letters **8**(2): 420-424.

Leung, P. H., et al. (2009). "Chemical properties and antioxidant activity of exopolysaccharides from mycelial culture of *Cordyceps sinensis* fungus Cs-HK1." Food Chemistry **114**(4): 1251-1256.

Lin, Y.-W. and B.-H. Chiang (2008). "Anti-tumor activity of the fermentation broth of *Cordyceps militaris* cultured in the medium of *Radix astragali*." Process Biochemistry **43**(3): 244-250.

Liu, H.-j., et al. (2011). "Morphological and microscopic identification studies of *Cordyceps* and its counterfeits." Acta Pharmaceutica Sinica B **1**(3): 189-195.

Lu, Y., et al. (2019). "Metabolic profiling of natural and cultured *Cordyceps* by NMR spectroscopy." Scientific reports **9**(1): 1-11.

Marie, R., et al. (2006). "Use of PLL-g-PEG in micro-fluidic devices for localizing selective and specific protein binding." Langmuir **22**(24): 10103-10108.

Nel, A. E., et al. (2009). "Understanding biophysicochemical interactions at the nano-bio interface." Nature materials **8**(7): 543-557.

Otsuka, H., et al. (2012). "PEGylated nanoparticles for biological and pharmaceutical applications." Advanced drug delivery reviews **64**: 246-255.

Oupicky, D., et al. (2002). "Importance of lateral and steric stabilization of polyelectrolyte gene delivery vectors for extended systemic circulation." Molecular Therapy **5**(4): 463-472.

Pekker, M. and M. Shneider (2014). "The surface charge of a cell lipid membrane." arXiv preprint arXiv:1401.4707.

Petros, R. A. and J. M. DeSimone (2010). "Strategies in the design of nanoparticles for therapeutic applications." Nature reviews Drug discovery **9**(8): 615-627.

Polakovič, M., et al. (1999). "Lidocaine loaded biodegradable nanospheres: II. Modelling of drug release." Journal of controlled release **60**(2-3): 169-177.

Rao, Y. K., et al. (2010). "Constituents isolated from Cordyceps militaris suppress enhanced inflammatory mediator's production and human cancer cell proliferation." Journal of ethnopharmacology **131**(2): 363-367.

Shrestha, B., et al. (2012). "The medicinal fungus Cordyceps militaris: research and

development." Mycological progress **11**(3): 599-614.

Tan, H.-Y., et al. (2018). "A multi-chamber microfluidic intestinal barrier model using Caco-2 cells for drug transport studies." PloS one **13**(5): e0197101.

Thanki, K., et al. (2013). "Oral delivery of anticancer drugs: challenges and opportunities." Journal of controlled release **170**(1): 15-40.

Tuli, H. S., et al. (2014). "Pharmacological and therapeutic potential of Cordyceps with special reference to Cordycepin." 3 Biotech **4**(1): 1-12.

Tuli, H. S., et al. (2013). "Cordycepin: a bioactive metabolite with therapeutic potential." Life sciences **93**(23): 863-869.

Ulleberg, E. K., et al. (2011). "Human gastrointestinal juices intended for use in in vitro digestion models." Food digestion **2**(1-3): 52-61.

Vashist, S. K., et al. (2012). "Nanotechnology-based biosensors and diagnostics: technology push versus industrial/healthcare requirements." Bionanoscience **2**(3): 115-126.

Wang, X., et al. (2001). "Synthesis, properties and biological activity of organotitanium substituted heteropolytungstates." Metal-based drugs **8**(4): 179-182.

Ways, M., et al. (2018). "Chitosan and its derivatives for application in mucoadhesive drug delivery systems." Polymers **10**(3): 267.

Xu, R., et al. (1992). "Effects of cordyceps sinensis on natural killer activity and colony formation of B16 melanoma." Chinese medical journal **105**(2): 97-101.

Yamaguchi, Y., et al. (2000). "Inhibitory effects of water extracts from fruiting bodies of cultured Cordyceps sinensis on raised serum lipid peroxide levels and aortic cholesterol deposition in atherosclerotic mice." Phytotherapy Research: An International Journal Devoted to Pharmacological and Toxicological Evaluation of Natural Product Derivatives **14**(8): 650-652.

Yamamoto, A., et al. (1994). "Effects of various protease inhibitors on the intestinal absorption and degradation of insulin in rats." Pharmaceutical research **11**(10): 1496-1500.

Yue, K., et al. (2013). "The genus Cordyceps: a chemical and pharmacological review." Journal of Pharmacy and Pharmacology **65**(4): 474-493.

Yue, Z.-G., et al. (2011). "Surface charge affects cellular uptake and intracellular trafficking of chitosan-based nanoparticles." Biomacromolecules **12**(7): 2440-2446.

Zhao-Long, W., et al. (2000). "Inhibitory effect of Cordyceps sinensis and Cordyceps militaris on human glomerular mesangial cell proliferation induced by native LDL." Cell Biochemistry and Function: Cellular biochemistry and its modulation by active agents or disease **18**(2): 93-97.

Zhao, Y.-N., et al. (2017). "A drug carrier for sustained zero-order release of peptide therapeutics." Scientific reports **7**(1): 5524.

Zheng, P., et al. (2012). "Genome sequence of the insect pathogenic fungus Cordyceps

militaris, a valued traditional Chinese medicine." Genome biology **12**(11): R116.





จุฬาลงกรณ์มหาวิทยาลัย
CHULALONGKORN UNIVERSITY

VITA

NAME WARUT KENGKITTIPAT

DATE OF BIRTH 5 DEC 1992

PLACE OF BIRTH BANGKOK, THAILAND

INSTITUTIONS ATTENDED FACULTY OF PHARMACEUTICAL SCIENCES,
CHULALONGKORN UNIVERSITY

HOME ADDRESS 1415/256 PHAHOLYOTHIN ROAD, SAMSENNAI,
PHRAYATHAI, BANGKOK, THAILAND 10400



จุฬาลงกรณ์มหาวิทยาลัย
CHULALONGKORN UNIVERSITY